

# Spatial deconvolution of 3-D diffuse optical tomographic image time series: Influence of background medium heterogeneity

Yong Xu, Harry L. Graber, Randall L. Barbour

Department of Pathology, SUNY Downstate Medical Center, 450 Clarkson Avenue, Box 25, Brooklyn, NY 11203 US  
[yong.xu@downstate.edu](mailto:yong.xu@downstate.edu)

**Abstract:** The ability of a spatial deconvolution algorithm to enhance reconstructed optical tomographic image quality was previously demonstrated. Here, additional computational studies show that introduction of complex medium geometry actually can improve the method's performance.

©2006 Optical Society of America

**OCIS codes:** (100.6950) Tomographic image processing; (100.6890) Three-dimensional image processing; (100.2980) Image enhancement; (100.1830) Deconvolution.

## 1. Introduction

Here we build upon previous demonstrations that the relatively low spatial resolution and quantitative accuracy of recovered optical parameters, in diffuse optical tomographic images reconstructed by linear perturbation approaches is primarily a result of linear convolution of spatial information [1-4]. A deconvolution algorithm, based on temporal encoding of spatial information, was developed that was shown to significantly improve qualitative and quantitative image accuracy, with a computational effort far lower than that required for recursive iterative reconstruction techniques [1]. Subsequent refinements of the deconvolution procedure have proved capable of performing equally well for 3-D imaging problems [2], and in restricted-view cases [3], and it has been shown that the tradeoff between enhancement of spatial information and degradation of temporal accuracy can be contained within acceptable bounds [4].

A potential limitation of the earlier work is that they examined only cases where the target medium consisted of a number of convex inclusions embedded in a homogeneous background. An intuitively plausible argument can be advanced, to the effect that the positive results presented in earlier reports are highly sensitive to the spatial extent of the mismatch between the optical parameters of the medium used for generating a deconvolution operator, or filter, and those of the medium to which the filter is subsequently applied. Similar arguments can be raised, regarding the sensitivity of deconvolution's effectiveness to increasingly complex parameter spatial distributions and to increasingly irregular external geometries. This report presents results of our examinations of these issues.

## 2. Methods

The medium geometry used for the studies, which was derived from a T1-weighted MRI of a human head, is shown in Figure 1. Line segments in Fig. 1 are edges of FEM mesh elements for the fine mesh used to compute target-

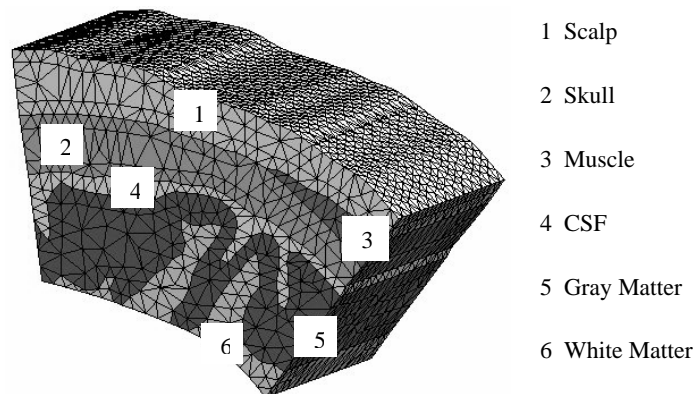


Fig. 1. Structure of three-dimensional medium used for all deconvolution characterization computations. Modeled tissue type 7, an inclusion ("tumor") embedded in the gray matter, is not visible in this exterior view.

medium detector data; coarser meshes are used for the computations of image reconstruction and deconvolution filters [2-4]. The absorption coefficient  $\mu_a$  of the gray matter and inclusion were dynamic, varying over time in the manners indicated in Figure 2, while the other five regions were static. Spatially complex static background optical

parameter heterogeneity was introduced by modifying the  $\mu_a$  and scattering coefficient  $\mu_s$  of the CSF region, as summarized in Table 1. Finally, the optical parameters of the inclusion were  $\mu_a = 0.24 \text{ cm}^{-1}$  (dynamic, in the manner indicated in Fig. 2) and scattering coefficient  $\mu_s = 10 \text{ cm}^{-1}$  (static).

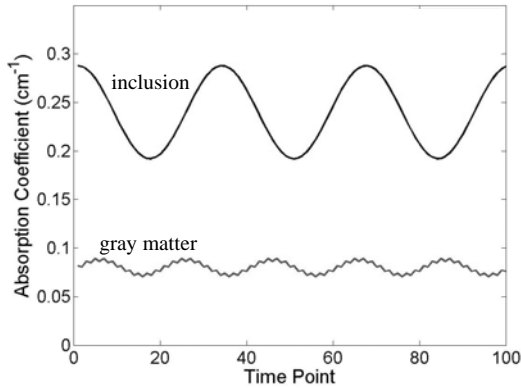


Fig. 2. Time dependence of  $\mu_a$  in the dynamic regions of the medium shown in Fig. 1.

Table 1. Time-averaged optical parameter values for medium regions 1-6.

Disparity level	CSF		Other non-tumor tissues	
	$\mu_a \text{ (cm}^{-1}\text{)}$	$\mu_s \text{ (cm}^{-1}\text{)}$	$\mu_a \text{ (cm}^{-1}\text{)}$	$\mu_s \text{ (cm}^{-1}\text{)}$
Case/Filter 1	0.08	10.0	0.08	10.0
Case/Filter 2	0.04	5.0	0.08	10.0
Case/Filter 3	0.01	1.0	0.08	10.0
Case/Filter 4	0.005	0.5	0.08	10.0

Descriptions of the procedures used for computing solutions to the diffuse optical tomography forward and inverse problems, generating deconvolution filters, and applying the latter, are found in Refs. 1-4. Filters (inclusion absent) and detector-readings time series (inclusion present) were computed for each of the four sets of time-averaged optical parameters listed in Table 1. To examine the sensitivity of the image enhancement algorithm to a complex mismatch between the spatial distributions of optical parameters of the filter-generating and target media, every deconvolution operator was applied to the image time series reconstructed from each medium's detector data. Spatial and temporal correlations were computed, between the true properties of each target medium case and all (with or without deconvolution) of the corresponding image time series.

### 3. Results

The location, size and shape of the inclusion region is shown in Figure 3(a); to illustrate the effectiveness of deconvolution at improving location and spatial resolution, representative reconstructed images, for Case2/Filter2 before (Fig. 3(b)) and after (Fig. 3(c)) also are shown. (The threshold value in 3(b) and 3(c) is  $\sim 50\%$  of the maximal image  $\mu_a$ , and is a reasonable limit because the time-average  $\mu_a$  of the inclusion is three times larger than that of the other tissue types.) In addition to the qualitative improvement apparent in 3(c), the latter also is significantly better in terms of quantitative accuracy (not shown). The spatial correlation between target medium and reconstructed image is shown, over the entire modeled time course, and for images obtained before and after application of the deconvolution filter, in Figure 4(a). It is seen there that the medium dynamics have a minimal impact on the degree

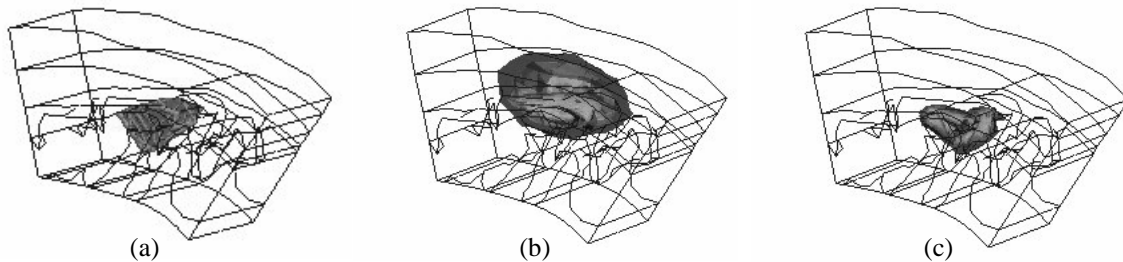


Fig. 3. (a) Location, size, shape of inclusion region in target medium. (b) Region where inclusion is recovered in first-order reconstructed image, at a selected time frame. (c) Region where inclusion is recovered in the spatially deconvolved image, at the same time frame as in 3(b).

of qualitative enhancement achieved. However, the particular deconvolution operator (Filter2) used here can produce unsatisfactory results if the disparity between the filter-generating and target medium grows too large, as shown by the spatial correlation vs. time curves in Figure 4(b). The complete set of spatial correlations between image and target medium time series, for all Case/Filter pairings and before and after deconvolution, are given in Table 2; a qualitatively similar trend is seen in the temporal correlations (not shown), although the latter typically are larger (average spatial correlation, before deconvolution, is 0.3492, while the corresponding average temporal correlation is 0.9252). A distinctive asymmetry is revealed in the effectiveness of filters applied to mismatched

target media, with Filter3 and Filter4 performing about equally well for all Cases, while Filter1 and Filter2 are ineffective when applied to the Cases having the greatest dissimilarity between filter-generating and target media.

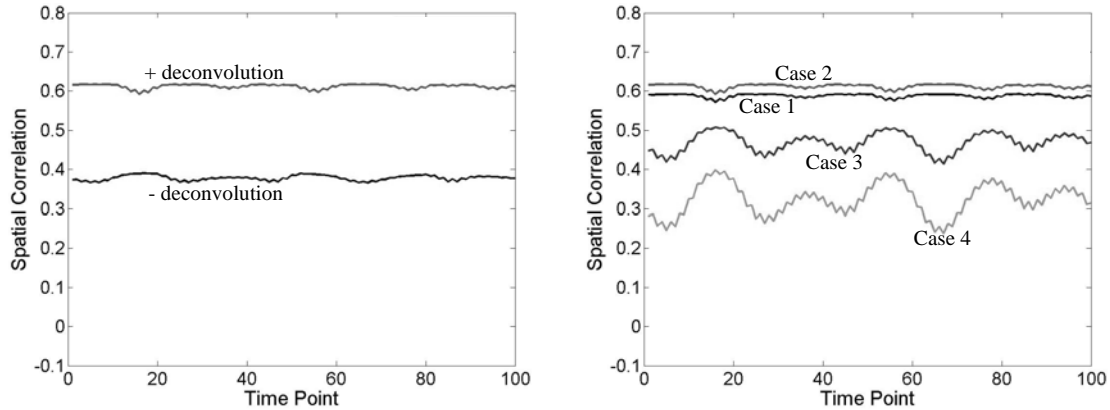


Fig. 4. (a) Spatial correlation vs. time for the Case 2 medium, before (-deconvolution curve) and after (+deconvolution) application of Filter2. (b) Spatial correlation vs. time, following image deconvolution, for Case1/Filter2, Case2/Filter2, Case3/Filter2, and Case4/Filter2 pairings.

Table 2. Time-averaged spatial correlations between image and target-medium time series, for all Case/Filter pairings and before and after spatial deconvolution.

	Filter 1		Filter 2		Filter 3		Filter 4	
	-	+	-	+	-	+	-	+
Case 1	0.3390	0.5408	0.3691	0.5881	0.3534	0.5113	0.3153	0.4748
Case 2	0.3447	0.4976	0.3782	0.6123	0.3634	0.5272	0.3244	0.4847
Case 3	0.3334	0.1543	0.3760	0.4628	0.3683	0.5535	0.3295	0.5056
Case 4	0.3244	0.0206	0.3713	0.3228	0.3679	0.5488	0.3294	0.5081

#### 4. Discussion

The principal objective result of these studies is a surprising finding that the quality of the deconvolved image is more robust in cases where the filter-generating and target media are strongly heterogeneous than when they are largely homogeneous. Secondly, while in general the existence of a significant disparity between these media does *not* guarantee that the deconvolved image is qualitatively inaccurate, there is a possibility of this occurring. Consequently, any step that can be reliably taken to increase the agreement between them does confer greater confidence in the accuracy of the deconvolved image. Here this was primarily accomplished by using an MRI-based anatomical prior as a scaffold for complex heterogeneous spatial distributions of optical parameters.

While the preceding strategy would typically be practicable in clinical contexts, we have developed, in parallel, an effective and computationally efficient alternative procedure that can produce results comparable to those for the matched Case/Filter pairings even in the absence of an anatomical prior. This method, which is completely described in the full-length report on these studies, makes use of a nonlinear reconstruction algorithm such as those in Refs. 1,3. In our implementation, however, the additional computational effort need be undertaken only once and can be performed independently of any optical tomographic data collection effort. Because of this, our ability to reconstruct spatially accurate image time series is not impaired. A further benefit of this more computation-intensive procedure is that it allows a single anatomical prior to serve as a template for optical tomographic imaging of many, unrelated individuals.

Additionally, the full set of filter performance characterizations included consideration of the impact of noise, in a manner similar to the studies reported in Ref. 4.

#### 5. References

- [1] R. L. Barbour, H. L. Graber, Y. Xu, Y. Pei, and R. Aronson, "Strategies for imaging diffusing media," *Transport Theory and Statistical Physics* **33**, 361-371 (2004).
- [2] H. L. Graber, Y. Xu, Y. Pei, and R. L. Barbour, "Spatial deconvolution technique to improve the accuracy of reconstructed three-dimensional diffuse optical tomographic images," *Applied Optics* **44**, 941-953 (2005).
- [3] Y. Xu, H. L. Graber, Y. Pei, and R. L. Barbour, "Improved accuracy of reconstructed diffuse optical tomographic images by means of spatial deconvolution: two-dimensional quantitative characterization," *Applied Optics* **44**, 2115-2139 (2005).
- [4] Y. Xu, Y. Pei, H. L. Graber, and R. L. Barbour, "Image quality improvement via spatial deconvolution in optical tomography: Time-series imaging," *J. Biomedical Optics*, Vol. 10, 051701 (2005).